

Jiayi Li¹, Xinyi Wang², Jichang Chen¹, Jun Jiao³, Mingbo Tong¹ & Chuliang Yan⁴

¹Nanjing University Of Aeronautics And Astronautics, Nanjing, China
 ²Shanghai Electro-Mechanical Engineering Institute, Shanghai, China
 ³China Special Vehicle Research Institute, Wuhan, China
 ⁴Beijing University Of Aeronautics And Astronautics, Beijing, China

Abstract

The process of aircraft forced water ditching involves complex nonlinear two-phase flow problems. Simple theoretical methods cannot obtain accurate results, and the experimental process is costly and has too many unstable factors. Therefore, the large eddy simulation method (LES) is used combined with the global dynamic grid strategy is used to numerically study the relevant phenomena in the aircraft water ditching problem. The main research object of this article is the suction force effect of the fuselage which will cause uneven distribution of load at the bottom of the aircraft, leading to changes in the aircraft's attitude, causing great instability and affecting the safety of plane in emergency. This research provides a reference for the analysis of aircraft load in different ditching scenarios.

Keywords: aircraft ditching, LES, VOF method, suction effect

1. Introduction

With the rapid development of the aviation industry, the range and volume of aircraft have increased simultaneously, and the execution of cross water flight tasks has become increasingly frequent. The emergency avoidance capability of civil aircraft has become a major research object. The causes of accidents causing forced landing on water include: human factors, fuel depletion, engine failure, engine damage and adverse weather conditions [1].

The airworthiness regulations stipulate the loading conditions during emergency landing of aircraft, requiring that the damage to the aircraft structure after impact is limited throughout the entire process, in order to minimize the risk of passenger injury and allow sufficient floating time for safe evacuation. Both the Federal Aviation Administration (FAA) and the European Aviation Safety Agency (EASA) have stated that it is necessary to study the possible behavior of aircraft during water landing through model testing or comparison with similar configurations of aircraft with known forced landing characteristics. The Civil Aviation Administration Regulations of China CCAR-25-R3 also have similar provisions on emergency landing performance. Therefore, conducting forced landing research on civil aircraft is an essential step for obtaining airworthiness certificates.

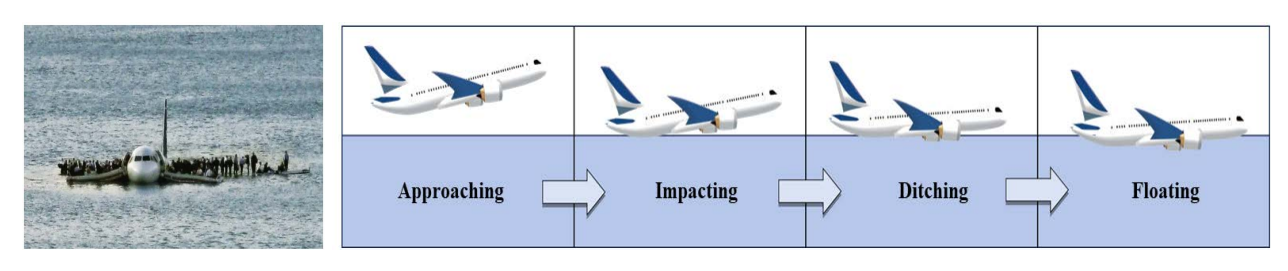


Figure 1 – Hudson River emergency ditching and four stages in water ditching

As shown in the Figure 1, during the planned surface emergency ditching process, the impact phase is the stage where the aircraft is subjected to the most severe load and is most prone to accidents. Compared with ground landing, the structural load characteristics of the aircraft body during ditching are affected by the deformation of the free liquid surface, resulting in different force and energy absorption characteristics of the aircraft bottom structure. Therefore, it is necessary to study the characteristics of the impact stage of aircraft water ditching.

During the impact phase, the aerodynamic and hydrodynamic loads of the aircraft are coupled with each other, resulting in complex water vapor effects at the tail of the fuselage. The suction effect refers to the formation of a low-pressure or even negative pressure zone at the rear of the fuselage when it comes into contact with water, producing a torque that causes the nose of the aircraft to tilt upwards. Due to the suction effect, the aircraft raises its head upwards, causing a rapid decrease in aerodynamic force and torque, and resulting in a change in its posture. It changes from slightly raising its head upwards before landing in contact with water to a nose dive, with the front fuselage hitting the water surface, which may cause serious damage to the front fuselage and the danger of the aircraft nose diving into the water.

Up to now, research on the influence of suction during aircraft water ditching mainly includes: In 2004, Pentecote P used the Smoothed Particle Hydrodynamics (SPH) method to study the multi-field coupling problem of a rigid aircraft water crash [2]. The analysis results showed that the influence of the suction generated by the aircraft bottom on the results cannot be ignored. In 2006, Clement H used the SPH method to simulate the water emergency landing of CN235-300M aircraft [3]. The article points out that the suction (negative pressure) that occurs at the rear of the aircraft during the forced landing process has a significant impact. In 2007, Streckwall H numerically simulate the process of aircraft fuselage ditching on static water [4]. The numerical results were in good agreement with experimental data, and it was pointed out that the high pressure in the front and negative pressure in the rear of the fuselage generated upward and downward forces, leading to the deceleration and pitch motion of the aircraft. In 2009, Nathalie used the SPH method to conduct numerical simulations on two scenarios of considering and not considering suction during aircraft water emergency landing, and provided comparative results [5]. It is pointed out in the article that suction plays a significant role in the motion of an aircraft during a ditching on water, and the attitude and speed of the aircraft are significantly affected. Due to the inability of the SPH method to simulate suction, suction is artificially applied in all operating conditions. Qu Q used VOF method and Fluent software to simulate the forced landing process of ARJ21 aircraft on calm water surface [6], capturing the deformation of the water surface well and proposing the optimal forced landing attitude. Zhang T based on MSC Dytran software uses the general coupling method to establish a coupling relationship between the Euler and Lagrangian parts of the model [7], and simulates the tail suction and head up phenomena during the forced landing process. It is proposed that compared with the SPH method, the general fluid structure coupling method does not require artificial suction. In 2016, Lu Z used the SPH method to couple the Navier-Stokes equation and a six degree of freedom model to numerically study the landing characteristics of three-dimensional helicopter models with different landing angles [8]. They simulated the forced landing process of complex helicopter models with vertical and forward speeds, solving the problem that the SPH method cannot simulate suction. In 2022, Spinosa E used the unsteady Reynolds-averaged Navier-Stokes equations method to study the hydrodynamic problems of three different types of fuselage in constant velocity fixed attitude motion in water [9]. They analyzed the pressure changes on wet surfaces and the characteristics of free surfaces. A negative pressure zone appeared at the rear where the longitudinal curvature of the fuselage changed, generating suction from a pure fluid power source.

In order to analyze the motion characteristics of aircraft in the scenario of ditching on calm water, this paper studies the suction force effect and water spray characteristics during the ditching by using the LES method. By comparing the clam water ditching results of three types of aircraft fuselage, analyzed the forces on the bottom of the fuselage and the splashing shape on both sides, as well as the generation and regularity of the suction effect at the tail of the fuselage.

2. Numerical Methods

The motion of the fuselage follows three fundamental laws: conservation of mass, conservation of momentum, and conservation of energy. In practical application scenarios, the speed of aircraft ditching is much lower than the speed of sound. Therefore, this article does not consider the fluid compressibility and assumes the fluid as an incompressible constant density fluid. Based on the assumption of incompressible flow, the energy conversion caused by temperature changes can be ignored, so the flow field only involves the laws of mass conservation and momentum conservation. The incompressible continuity equation can be written as:

$$\frac{\partial u}{\partial x} + \frac{\partial v}{\partial y} + \frac{\partial w}{\partial z} = 0 \tag{1}$$

The law of conservation of momentum states that the rate of change of the momentum of a fluid in a cell over time is equal to the sum of all external force vectors acting on the cell. When solving any fluid flow problem, the law of conservation of momentum should be satisfied. Under the premise of incompressible fluid, its specific form is:

$$\frac{\partial u}{\partial t} + u \frac{\partial u}{\partial x} + v \frac{\partial u}{\partial y} + w \frac{\partial u}{\partial z} = -\frac{1}{\rho} \frac{\partial p}{\partial x} + v \left(\frac{\partial^2 u}{\partial x^2} + \frac{\partial^2 u}{\partial y^2} + \frac{\partial^2 u}{\partial z^2} \right) + f_x$$

$$\frac{\partial v}{\partial t} + u \frac{\partial v}{\partial x} + v \frac{\partial v}{\partial y} + w \frac{\partial v}{\partial z} = -\frac{1}{\rho} \frac{\partial p}{\partial y} + v \left(\frac{\partial^2 v}{\partial x^2} + \frac{\partial^2 v}{\partial y^2} + \frac{\partial^2 v}{\partial z^2} \right) + f_y$$

$$\frac{\partial w}{\partial t} + u \frac{\partial w}{\partial x} + v \frac{\partial w}{\partial y} + w \frac{\partial w}{\partial z} = -\frac{1}{\rho} \frac{\partial p}{\partial z} + v \left(\frac{\partial^2 w}{\partial x^2} + \frac{\partial^2 w}{\partial y^2} + \frac{\partial^2 w}{\partial z^2} \right) + f_z$$
(2)

Each term in the momentum conservation equation represents a force acting on the fluid cell, and the external forces acting on the cell include pressure, viscous force and volumetric force. P is the pressure acting on the microelements of the fluid system, v is the kinematic viscosity of the fluid. In order to simulate the complex changes in water flow at the tail end, the WALE sub grid scale model in the large eddy simulation method is adopted. The basic equation is:

$$S_{ij}^{d} = \frac{1}{2} \left(\overline{g}_{ij}^2 + \overline{g}_{ji}^2 \right) - \frac{1}{3} \delta_{ij} \overline{g}_{kk}^2 \tag{3}$$

In the above equation δ_{ij} is the Kronecker symbol, \overline{g}_{ij} is the velocity gradient tensor, \overline{g}_{ij} and \overline{g}_{ij}^2 can be written as:

$$\overline{g}_{ij} = \frac{\partial \overline{u_i}}{\partial x_j}
\overline{g}_{ij}^2 = \overline{g}_{ik} \overline{g}_{kj}$$
(4)

In the WALE model, the sub grid scale turbulent kinetic energy viscosity is represented by the following mixing length type formula:

$$v_{t} = L_{s}^{2} \frac{\left(S_{ij}^{d} \cdot S_{ij}^{d}\right)^{3/2}}{\left(\overline{S_{ij}} \cdot \overline{S_{ij}}\right)^{5/2} + \left(S_{ij}^{d} \cdot S_{ij}^{d}\right)^{5/4}}$$
(5)

 L_s is a length scale, expressed as:

$$L_s = min\left(\kappa d, C_w \triangle\right) \tag{6}$$

Compared with other liquid level capture methods, the VOF method is simple and easy to implement. It has good stability and meets the calculation accuracy requirements. At the same time, it has the advantage of occupying less memory. Therefore, this article uses the VOF method to accurately capture the liquid level. The volume fraction function of the VOF method is as follows:

$$a_i = \frac{V_i}{V}. (7)$$

Among them, V_i and V respectively represent the volume of fluid in the unit grid and the volume of the grid itself. When $a_i=1$, it means that all the fluid in the grid cell is present. When $a_i=0$, it means all other fluid phases are present within the grid cell. When $0 < a_i < 1$, it means the grid element was an interface element containing multiphase fluids.

At present, adaptive mesh refinement (AMR) technology can be divided into three types based on different grid refinement methods: 1. r-type refinement by adjusting grid nodes to ensure the overall quality of the grid remains unchanged. 2. h-type refinement by segmenting local unit grids to improve local area resolution. 3. p-type refinement by adding interpolation nodes to the computational domain and approximating the flux on the grid interface using higher-order polynomials to obtain higher accuracy solutions. Due to the fact that the research object of this article is the suction effect during the ditching process, there is a high resolution requirement for the local water air two-phase flow interface. Therefore, the p-type grid plan is the most suitable.

Based on the above adaptive method, the mesh near the free liquid surface will gradually refine during the iteration process to achieve fine surface capture function, as shown in Figure 2, is the continuous local refinement process around the interface of two-phase flow.

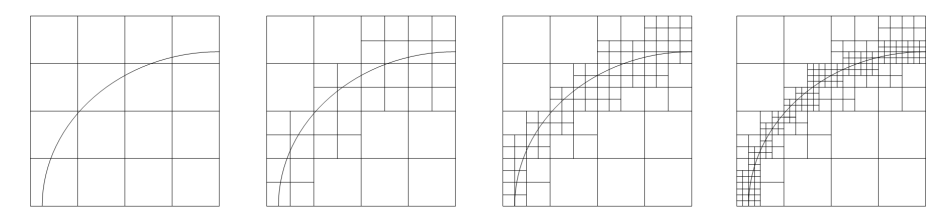


Figure 2 – Mesh refinement steps near the interface

2.1 Aircraft Ditching Model

For emergency water ditching of aircraft, the load on the bottom of the fuselage is an important factor affecting the structural integrity of the entire aircraft. Therefore, it is important to study the impact of different fuselage bottom structures. The research object of this article is three different types of aircraft fuselage: Modeling of the circular cross-section hyperbolic and circular elliptical cross-section hyperbolic fuselage in the landing test of the Italian National Research Council's Institute of Marine Engineering (CNR-INM) [10] and modeling of the NASA Langley Aviation Laboratory's NACA 57A ship type fuselage [11]. The analytical functions for the hyperbolic fuselage with circular cross-section and circular elliptical cross-section are shown in the following Figure 3:

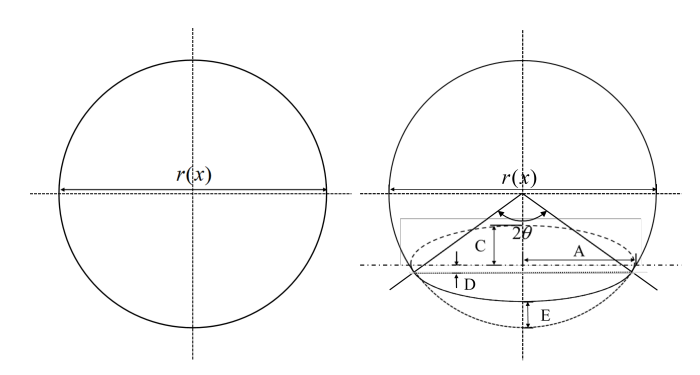


Figure 3 – Analytical functions for different cross-sections.Left:circular cross section,Right:circular-elliptical cross-section

Three simplified models for simulation are shown in the following Figure 4. To ensure the similarity of motion among the three types of aircraft ditching models, the length of all three aircraft models is 2.133m, and the grid size of the peripheral flow field domain is $13.8 \times 7 \times 7$ m. To reduce computational

complexity and improve computational efficiency, all models use semi models for computation. The total number of grid cells is 13 million. The schematic diagram of the calculated flow field domain is shown in the Figure 5:



Figure 4 – Three simplified models for simulation.Left:circular cross-section fuselage,middle:circular-elliptical cross-section fuselage,Right:NACA 57A fuselage

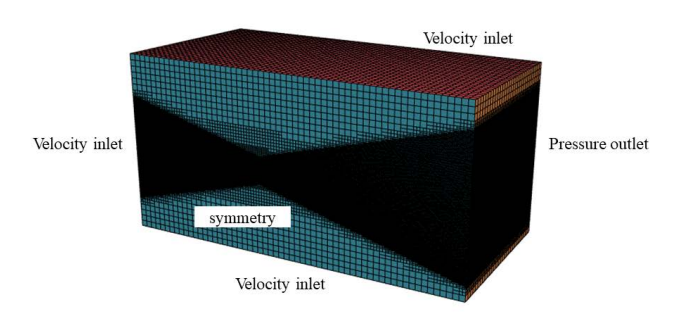


Figure 5 – Grid and boundary condition diagram

2.2 Model Applicability Verification

Referring to the hydrodynamic tests conducted by NASA's Langley Aeronautical Laboratory [11], the NACA 57A model with a V-shaped bottom buoy that used for a double buoy seaplane, was selected as the subsequent research object. Simulations were conducted on the static water surface sliding of the fuselage at six different speeds and compared with the experiments in the NACA-TN-716 report to verify the accuracy of the calculation method used in this paper.

The grid diagram used for the model and calculation of the NACA 57A fuselage is shown in the following Figure 6. The mesh near the free liquid surface has been densified, with an overall mesh volume of approximately 8.89 million and a minimum mesh size of 0.005m, with y+ taking 1.

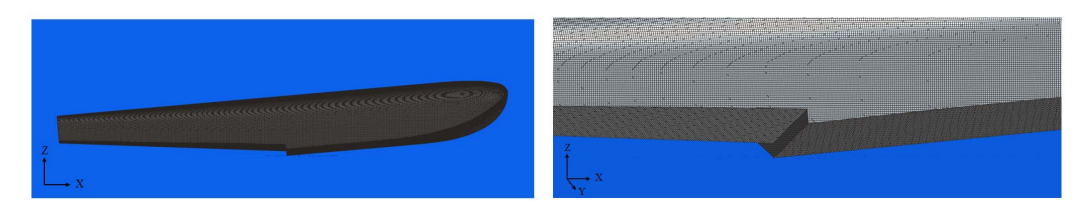


Figure 6 - Grid diagram of static water surface sliding case

The drag of the fuselage and the displacement in the z-direction are shown in the following Figure 7. From the overall trend of changes, the results of both are in good agreement with the experimental data, respectively. It can be seen that the calculation method selected in this article is reliable.

3. Results and Analysis

3.1 Influence of Fuselage Shape

This section mainly introduces the comparison of ditching results of three aircraft body shape models under the conditions of forward flight speed of 6m/s, sinking speed of 0.9m/s, pitch angle of 5°. All models have been simplified and the calculation process does not include the influence of the wings. Therefore, hydrodynamics is the main force during the entire ditching process.

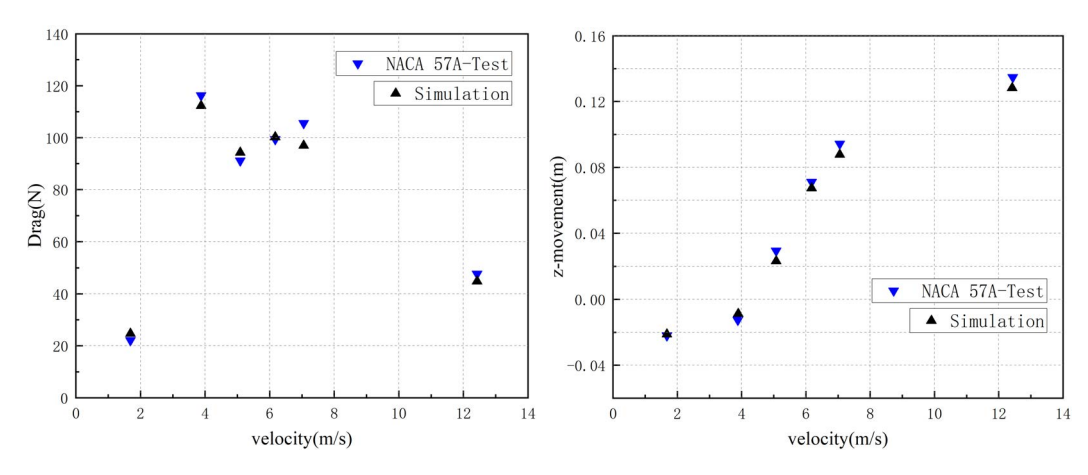


Figure 7 – Comparison between simulation and experimental results of NACA 57A fuselage model (Left: Drag, Right: z-direction displacement)

In order to clearly observe the changes in water surface during ditching, the volume fraction of the water phase and the pressure contour at the bottom of the fuselage were recorded at 25ms, 50ms, and 75ms after contact with the water surface. The calculation results of the three models are shown in the following Figure 8-10.

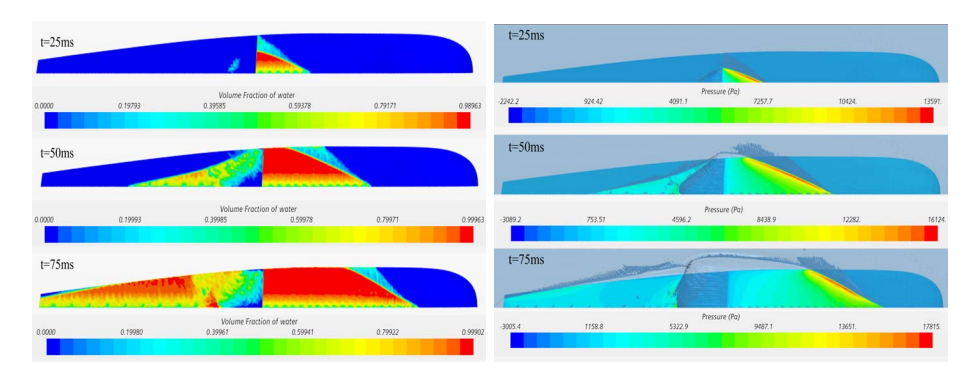


Figure 8 – NACA 57A fuselage calculation results (Left: Volume fraction of water, Right: Bottom pressure)

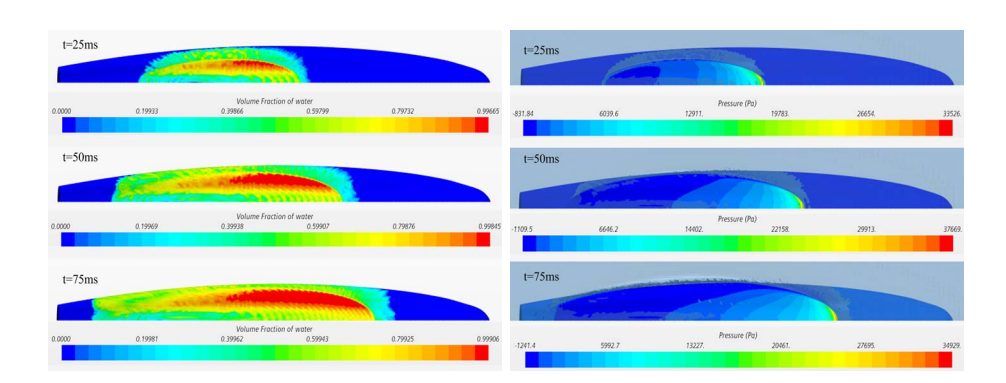


Figure 9 – Circular cross-section hyperbolic fuselage calculation results (Left: Volume fraction of water, Right: Bottom pressure)

Due to the collision between the fuselage and the water surface during the ditching process, the air that didn't have a chance to escape forms a regular arrangement of bubbles at the bottom of the fuselage, creating an air cushion effect, as shown in the Figure 8. As the rear fuselage touches the water, bubbles arranged in a regular pattern also form at the bottom. Comparing the air cushion effect of the front and rear fuselage, it can be found that the bubbles in the front fuselage are smaller and denser than those in the rear fuselage, it shows a tendency to dissipate diagonally towards the rear.

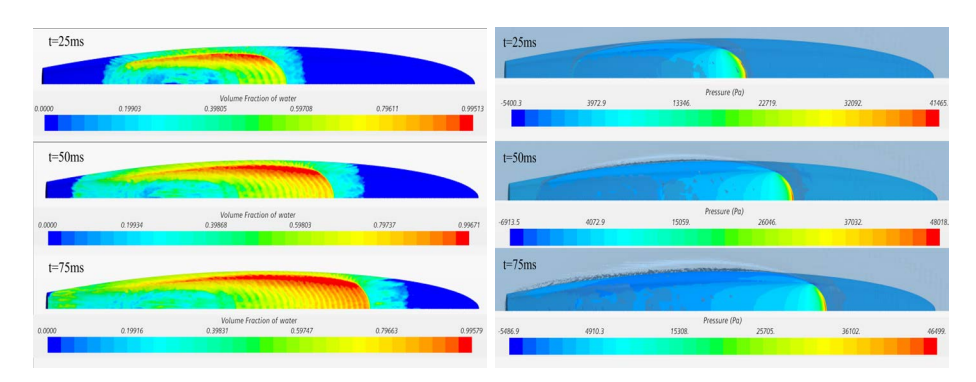


Figure 10 – Circular-elliptical cross-section hyperbolic fuselage fuselage calculation results (Left: Volume fraction of water, Right: Bottom pressure)

From the velocity contour, it can also be inferred that this is due to the faster water phase velocity in the front fuselage. During the process of ditching, the maximum pressure is always at the contact point between the fuselage and the water. The pressure gradually decreases from the contact point to the breaking step point, then reaches the minimum value in the rear cavity of the fuselage step. It can also be seen from the Figure 8 that the low-pressure area at this point sucks some water into the cavity and impacts the bottom surface of the fuselage. From an overall perspective, the broken step and some areas at the rear belong to the low-pressure area at the bottom of the fuselage, while the water contact area at the front of the fuselage belongs to the high-pressure area. The high-pressure area at the front and the low-pressure area at the broken step work together to produce a suction effect.

As shown in Figure 8-10, comparing the three different fuselage, the volume fraction of the air phase in the landing area of the NACA 57A fuselage is significantly smaller than the other two. The circular-elliptical cross-section fuselage has the most air phase at the bottom, this is mainly due to its flatter bottom compared to the other two, which will result in slower air escape speed. Therefore, the flatter the bottom of the fuselage, the more significant the air cushion effect will be, and the hull shape design can significantly alleviate this phenomenon. However, due to the presence of a step, there will also be an air chamber after the step.

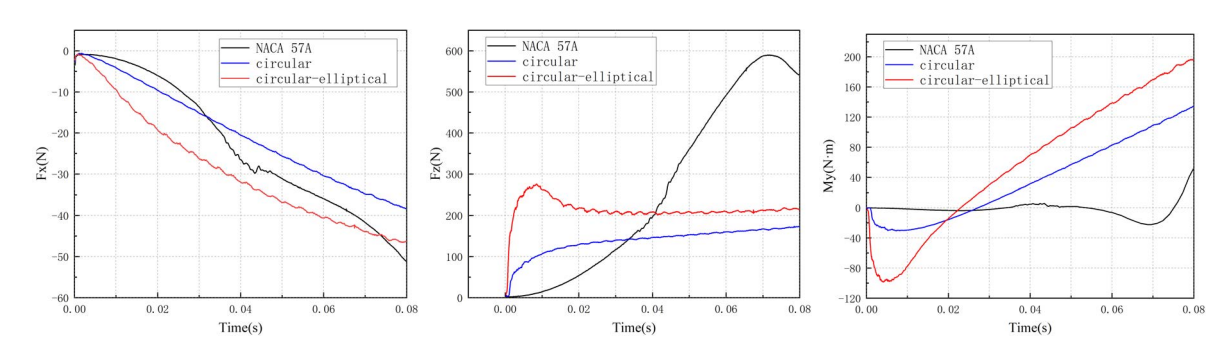


Figure 11 – Three types of fuselage force time history diagrams (Left: X-direction drag, Middle: Z-direction buoyancy, Right: Pitching moment)

As shown in Figure 11, at this forward flight speed, the lateral drag values of the three different fuselage during the ditching process are approximately similar. Within the time range of 0-32ms the NACA 57A fuselage experiences the smallest drag value, but it increases the fastest in the subsequent process. For the NACA 57A fuselage, its wet area is always smaller than the two hyperbolic fuselages. Therefore, in the early stage of ditching, the horizontal drag of the NACA 57A fuselage is the smallest. As the exercise progresses, the presence of cavities in the step leads to more intense interaction between the water and gas phases after the step, and some backflow water bodies attack the fuselage. Therefore, the horizontal drag of the NACA 57A fuselage increases rapidly. But for the other two types of cross-sectional fuselage, because the difference in lateral projection area is not significant, the trend of drag change is basically the same.

There are significant differences in the variation of vertical impact force during the ditching of three different shapes of aircraft. The changes in the two hyperbolic fuselages are similar. The pressure values near the contact point of the two hyperbolic fuselages in the early stage of landing are much higher than those of the NACA 57A fuselage, but in the subsequent process, the latter rapidly increases. There are significant differences in the torque changes experienced by three different shapes of fuselage during water movement. The suction effect of the two hyperbolic fuselages rapidly occurs after ditching, and gradually decreases until it disappears as the ditching motion further progresses.

On the other hand, the peak of vertical drag on the NACA 57A fuselage appeared later, and only produces a significant suction effect after a large area of water falls behind the step. The suction effect of the circular cross-section hyperbolic fuselage has the longest duration, followed by the circular elliptical cross-section hyperbolic fuselage, and the NACA 57A fuselage has the shortest duration. If the strength of the suction effect is reflected by the torque value, the suction effect of the NACA 57A fuselage is the smallest, followed by the hyperbolic fuselage with a circular cross-section, and the hyperbolic fuselage with a circular elliptical cross-section has the strongest suction effect.

3.2 Influence of Flight Speed

This section analyzes the results of water ditching at different forward flight speeds. Simulates the water ditching at 6m/s, 12m/s, and 20m/s.

As shown in the Figure 12-14, the volume fraction contour of the bottom water phase at different fuselage under three different speeds are shown. From left to right are the calculation results of the NACA57 fuselage, circular cross-section fuselage, and circular-elliptical cross-section fuselage, respectively. The forward flight speeds from top to bottom are 6m/s, 12m/s and 20m/s.

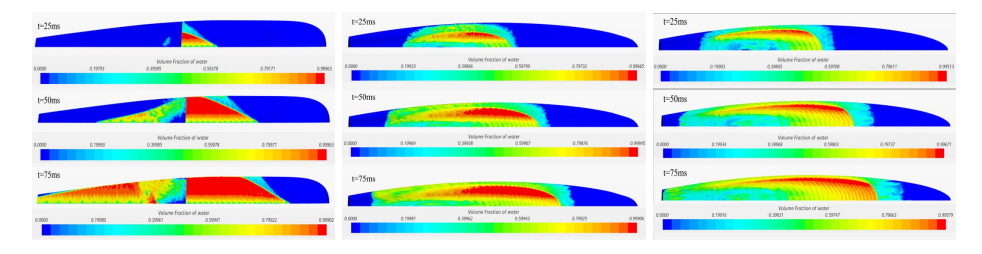


Figure 12 – Bottom phase diagram-volume fraction of water when forward flight speed is 6m/s (Left: NACA 57A fuselage, Middle: Circular cross-section hyperbolic fuselage, Right: Circular-elliptical cross-section hyperbolic fuselage)

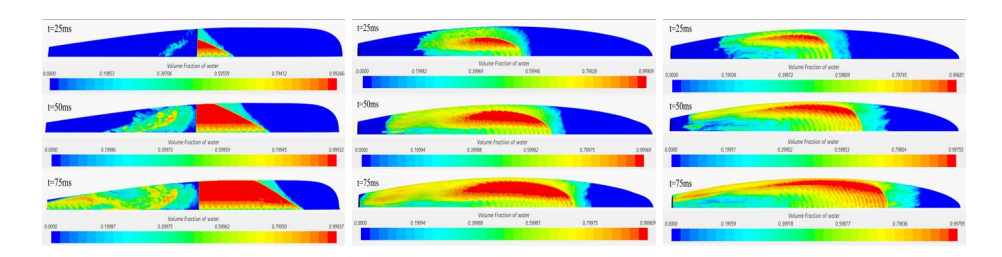


Figure 13 – Bottom phase diagram-Volume fraction of water when forward flight speed is 12m/s (
Left: NACA 57A fuselage, Middle: Circular cross-section hyperbolic fuselage, Right:
Circular-elliptical cross-section hyperbolic fuselage)

As shown in the Figures 12-14, the volume fraction of splashed water phase at the bottom of the fuselage increases, the air at the forefront of contact between the fuselage and the water surface decreases. The air cushion phenomenon gradually weakens and bubbles are more prone to breaking and escaping. At a fixed moment, the higher the forward flight speed, the larger the wet area of the fuselage, and the low-pressure area moves forward towards the fuselage, the smaller the minimum pressure value and the larger the maximum pressure value.

As shown in the Figures 15-17, as the forward flight speed increases, the phenomenon of wave jet splashing at the water contact point in the front of the fuselage and splashing at the rear of the

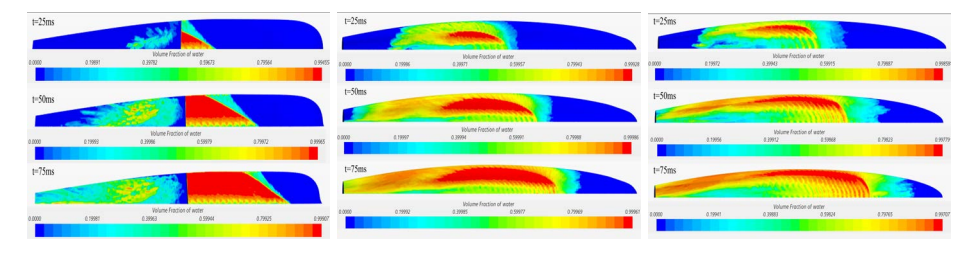


Figure 14 – Bottom phase diagram-volume fraction of water when forward flight speed is 20m/s (
Left: NACA 57A fuselage, Middle: Circular cross-section hyperbolic fuselage, Right:
Circular-elliptical cross-section hyperbolic fuselage)

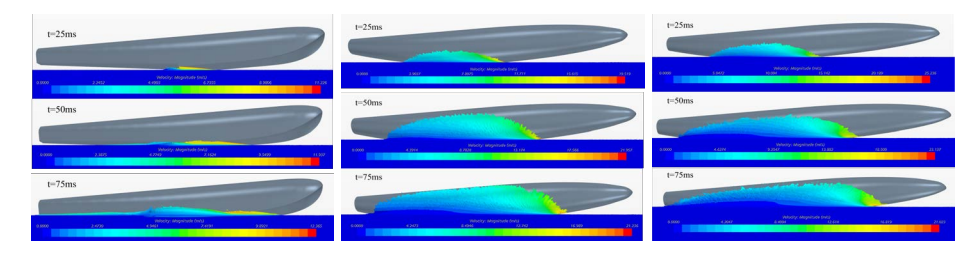


Figure 15 – Splashing situation when flying at a speed of 6m/s (Left: NACA 57A fuselage, Middle: Circular cross-section hyperbolic fuselage, Right: Circular-elliptical cross-section hyperbolic fuselage)

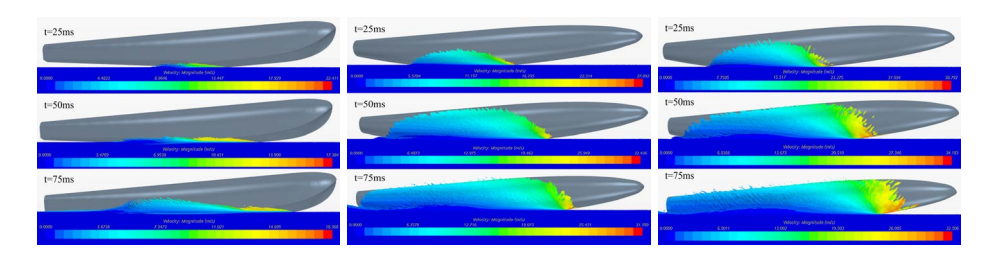


Figure 16 – Splashing situation when flying at a speed of 12m/s (Left: NACA 57A fuselage, Middle: Circular cross-section hyperbolic fuselage, Right: Circular-elliptical cross-section hyperbolic fuselage)

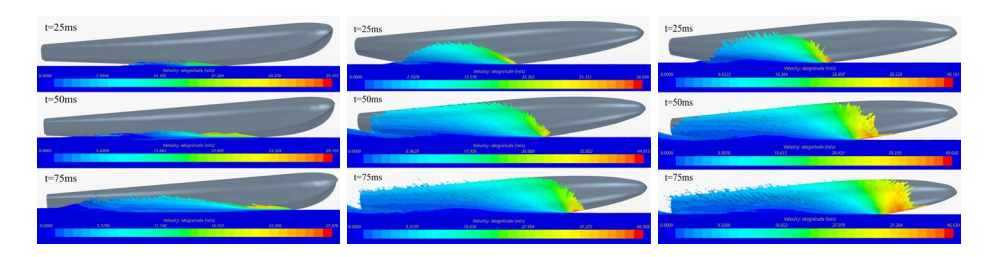


Figure 17 – Splashing situation when flying at a speed of 20m/s (Left: NACA 57A fuselage, Middle: Circular cross-section hyperbolic fuselage, Right: Circular-elliptical cross-section hyperbolic fuselage)

fuselage becomes more severe. The peak splashing speed and splashing height increase correspondingly, and the phenomenon of splashing height falling back is obvious.

Mean while, the duration of the suction effect when the fuselage lands on water is shorter, and the intensity of the tail suction effect is smaller. The suction effect of a large curvature fuselage ditching is more sensitive to the increase of forward flight speed and the variation of suction effect is greater. The NACA 57A fuselage has transitioned from a weak and strong tail suction effect at low forward flight speeds to a weak suction effect only once at high forward flight speeds. From the Figure 15-17, it can be seen that the step structure has a significant inhibitory effect on the splashing height on both sides of the fuselage, which can greatly reduce the damage to the structure.

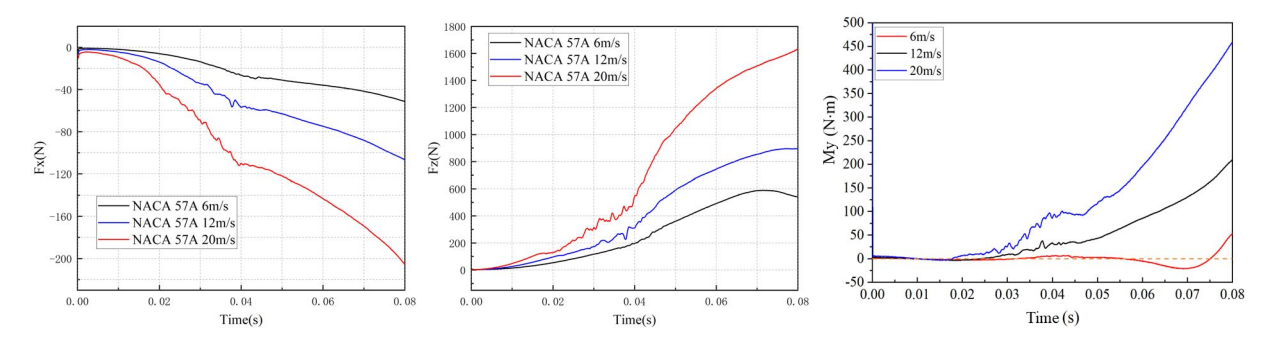


Figure 18 – Force on the NACA 57A fuselage (Left: X-direction drag, Middle: Z-direction buoyancy, Right: Pitching moment)

Taking the NACA 57A fuselage as an example, as the forward flight speed increases, the force and the moment both increase rapidly, as shown in Figure 18. Therefore, in emergency situations, it is necessary to strictly control the forward flight speed during ditching to prevent the aircraft from being subjected to forces beyond its capacity, or damage to other aircraft structures caused by excessive splashing of water on both sides of the aircraft.

4. Conclusion

This article uses three different fuselage for simulation of clam water ditching. The overall force process of the aircraft during the impact phase is analyzed. By observing the water phase distribution on the surface of the aircraft and the pressure distribution on the bottom, the influence of body shape and forward flight speed on the suction effect of the aircraft's water ditching is analyzed.

5. Acknowledgments

The research content of this article has been supported by Aeronautical Science Foundation of China, project number:20230023052001,20220023052001. Distinguished postdoctoral project of Jiangsu Province and Natural Science Foundation of Jiangsu Province (No.BK20241372)

6. Contact Author Email Address

Email address: lijiayii@nuaa.edu.cn

7. Copyright Statement

We confirm that we and our company or organization, hold copyright on all of the original material included in this paper. We also confirm that we have obtained permission, from the copyright holder of any third party material included in this paper, to publish it as part of their paper. We confirm that we give permission, or have obtained permission from the copyright holder of this paper, for the publication and distribution of this paper as part of the ICAS proceedings or as individual off-prints from the proceedings.

References

- [1] Tong M, Chen J and Li L. State of the art and perspectives of numerical simulation of aircraft structural integrity from hydrodynamics-PartI:Ditching and floating. *Acta Aeronautica et Astronautica Sinica*, Vol.42, No.5, pp 1-35, 2021.
- [2] Pentecte N, Kohlgrüber D. Crash on Water: a Highly Multi-Physics Problem. *EUROPAM2004, 14th European Conference and Exhibition on Digital Dimulation for Virtual Engineering*, Paris, Frankreich, Vol.10, pp 11-13, 2004.
- [3] Climent H, Benitez L and Rosich F. Pentecote. Aircraft Ditching Numerical Simulation. *25th International Congress of the Aeronautical Sciences*, Hamburg, Germany, pp:1-16, 2006.
- [4] Streckwall H, Lindenau O and Bensch L. Aircraft ditching: a free surface/free motion problem. *Archives of civil and mechanical engineering*, Vol.7, No.3, pp:177–190, 2007.
- [5] Toso N. Contribution to the Modelling and Simulation of Aircraft Structures Impacting on Water. *Dissertation of Doctoral Degree*, Stuttgart, University Stuttgart, 2009.

- [6] Qiulin Q, Peiqing L and Baodong G. Numerical Study on the Hydraulic Performance of Landing Impact of a Certain Type of Passenger Aircraft in Water Forced Landing. *Civil Aircraft Design and Research*, Vol.13, No.1, pp:64-69, 2009.
- [7] Zhang T, Li S and Dai H C. The suction force effect analysis of large civil aircraft ditching. *Sci China Tech Sci*, Vol.42, No.12, pp:1407-1415, 2012.
- [8] LU Z, XIAO T. Investigation of helicopter ditching angle on fuselage pressure load using a SPH method. *46thAIAA Fluid Dynamics Conference*, Reston, America, pp:3815, 2016.
- [9] Spinosa E, Broglia R and Iafrati A. Hydrodynamic analysis of the water landing phase of aircraft fuselages at constant speed and fixed attitude. *Aerospace science and technology*, No.130, pp:107846, 2022.
- [10] Iafrati A, Grizzi S. Cavitation and ventilation modalities during ditching. *Physics of Fluids*, Vol.31, No.5, pp:1-14, 2009.
- [11] John B.Parkinson, Roland E. Olson Hydrodynamic and Aerodynamic Tests of a Family of Models of Seaplane Floats with Varying Angles of Dead Rise -N.A.C.A. Models 57-A, 57-B, and 57-C. *NASA Technical Reports Server*,1939.